www.sciencemag.org/cgi/content/full/324/5930/1084/DC1

Supporting Online Material for

The Human K-Complex Represents an Isolated Cortical Down-State

Sydney S. Cash,* Eric Halgren, Nima Dehghani, Andrea O. Rossetti, Thomas Thesen, ChunMao Wang, Orrin Devinsky, Ruben Kuzniecky, Werner Doyle, Joseph Madsen, Edward Bromfield, Loránd Erőss, Péter Halász, George Karmos, Richárd Csercsa, Lucia Wittner, István Ulbert

*To whom correspondence should be addressed. E-mail: scash@partners.org

Published 22 May 2009, *Science* **324**, 1084 (2009)
DOI: 10.1126/science.1169626

This PDF file includes

The Human K-Complex Represents an Isolated Cortical Down-State

Supporting Online Material

Materials and Methods

Subjects. Eight patients (15-48 years old; 4 female) with long-standing pharmaco-resistant complex partial seizures participated after fully informed consent according to NIH guidelines as monitored by the local Institutional Review Boards. Simultaneous scalp, macroelectrode and microelectrode cortical recordings during natural sleep were made over the course of clinical monitoring for spontaneous seizures. Subdural grid and strip clinical electrode arrays were placed in order to confirm the hypothesized seizure focus, and locate epileptogenic tissue in relation to essential cortex, thus directing surgical treatment. Patients were all right-handed, with intelligence and personality in the normal range (see table S1 for clinical characteristics of individual patients). The decision to implant, the electrode targets and the duration of implantation were made entirely on clinical grounds without reference to this experiment. The patients were informed that participation in the experiment would not alter their clinical treatment in any way, and that they may withdraw at any time without jeopardizing their clinical care.

Probes. Macro-electrode contacts were 3mm platinum discs spaced 10mm center-to-center, embedded in 8x8 grid arrays, linear 1x8 strips or some combination thereof. Linear microelectrode arrays were placed perpendicular to the cortical surface within the hypothesized epileptogenic zone, passing ~3mm from the pial surface to the white matter, and recording en passant from the different lamina of a cortical column. Laminar microarrays consisted of 24 individual 90%Pt-10%Ir contacts, each 40μm in diameter and spaced 150μm center-to-center (*S1*). Electrodes were located relative to cortical gyri using intraoperative photographs, as well as CTs and MRIs taken with the probes in place. The depths of the laminar contacts below the pial surface are fixed and known because the top

of the probe is a silastic sheet that adheres by surface tension to the cortical surface. In addition, laminar contacts in gray matter, white matter, and CSF have characteristic activity patterns, assisting in resolution of their entry and exit points. In 3 cases the relationship of the probe to cortical lamina was confirmed with post-resection histological examination (example shown in fig. S1). Scalp EEG, electro-oculogram (EOG) and submental electromyogram (EMG) electrodes were placed to permit sleep staging (see below).

Recordings. Recordings from grid and strip macro-electrode arrays were made using 128 channel clinical cable telemetry systems with sampling rates between 200 and 800 Hz and bandpass from 0.1 to 100-400 Hz. These recordings were referenced to intradural electrodes facing away from the cortex. Recordings from microelectrode arrays used custom amplifiers in a differential configuration from 23 pairs of successive contacts, at 2 kHz (16 bit) sampling rate for field potentials and 20 kHz (12 bit) for unit activity, and stored continuously with stimulus and timing markers permitting synchronization with grid and strip recordings. Recordings were not analyzed if a patient had a seizure in the recording session, or if the local cortex exhibited chronic slow waves, interictal spikes or other frankly abnormal activity.

Estimation of population trans-membrane current flows and unit activity in different cortical layers. Population trans-membrane current flows were estimated using current source density (CSD) analysis (*S2*), calculated as the second spatial derivative of field potentials (0.5-30Hz) after applying a 5-point Hamming filter (*S1*) or by using the inverse CSD (iCSD) method of Pettersen et al. (*S3*). CSD may be due to either active transmembrane currents, or passive returns distributed according to the geometry of the cell. Active currents may be due to neurotransmitter-gated channels in the postsynaptic membrane, or to voltage-gated channels and other intrinsic membrane currents (*S4*). CSD analysis assumes that conductivity is uniform and isotropic in the tissue immediately

surrounding the probe (*S5*). This assumption has been tested in the hippocampus where deviations from the homogeneous approximation are too small to influence the spatial distribution of sources and sinks (*S6*).Variable electrode spacing or potential amplification could produce spurious CSD signals but these effects were evaluated experimentally in our system and were less than 5% (*S1*). CSD analysis will miss transmembrane currents if they do not result in a net radial extracellular current, as might happen if they are produced by synapses on a spherically symmetrical dendritic domain. CSD will also fail to detect currents that flow over distances that are small relative to the spatial sampling density. Modeling and experimental measures indicate that the center-to-center contact spacing of 150μm used in the current study is adequate to sample laminar CSD in macaque primary visual cortex (*S7, S8*). The limiting factor was the dendritic domains of stellate cells in thalamorecipient layer IVc. Cortex is thicker in humans, and the sampled areas are not known to have a thin but important sublayer comparable to IVc. Nonetheless, it is likely that the CSD analysis reported here is relatively insensitive to synaptic activity on layer IV stellate cells. Finally, current sources or sinks can be missed if the laminar probe does not sample the entire cortical depth. Multi-Unit Activity (MUA), an estimate of population neuronal firing, was calculated in each cortical layer by rectifying high frequency activity (300-5000 Hz) and smoothing with a 50 Hz low-pass filter (*S1*).

Time and frequency domain analysis were initially performed using Neuroscan Edit 4.3 software with spectral content of the LFP and CSD data evaluated using custom MatLab routines based on the EEGLAB package (*S9*). This approach is based on either a shorttime Fourier transform or sinusoidal wavelet transform. Both methods were tried without significant differences. The frequency changes were also evaluated using custom designed C++ and MatLab software (*S10, S11*) in which individual trial event-related spectral power (iERSP) was calculated by convoluting the single trial signal $s_i(t)$ for each channel i with complex Morlet's wavelets. In all cases, the resulting time-

frequency plots of spectral power were normalized with respect to an appropriate baseline (-500 to -100 ms before the K-complex) for each frequency and plotted as z-scores. There were no significant differences between the methods.

Sleep staging and grapho-element identification followed standard criteria and was verified by qualified raters. Sleep staging relied on direct behavioral observation, surface EEG (between one and four scalp electrodes referenced to the mastoid), EOG and submental EMG. Spontaneous KC were identified as multiphasic waves during Stage 2 sleep with a significant surface negative and then surface positive potential occurring ~500 and 900 ms from the beginning of the waveform. Stage 2 sleep was identified by observation of the patient's sleeping behavior as well as the absence of rapid eye movements, occasional delta activity (<20%), KC and spindles (*S12*).We also evoked KC during stage 2 sleep with simple auditory tones presented randomly (30-40s intervals) at an intensity that was gradually increased so that more than half of the tones evoked KC without eliciting arousal.

Histology of the region directly surrounding the recording electrode was obtained in 3 of the 8 patients. Two of those examinations revealed normal cortical neurons and layer architecture despite the presence of a dysplastic lesion in some other region. Figure S1 shows a photomicrograph of the tissue adjacent to one of these electrodes (Patient G). The third showed evidence of mild dysplasia. Inspection of pre-operative MRIs in 4 of the remaining 5 patients failed to show any structural abnormality in the region near the implantation. The fifth patient showed possible dysplastic tissue in the region of the array. Identical results were found in the two patients with evidence of dysplasia near the recording array compared to the other patients. An additional (ninth) patient was recorded but their data was rejected from consideration due the presence of obvious epileptiform activity. Therefore, the preponderance of data suggests that our recordings were done in relatively normal neuronal tissue and are unlikely to reflect pathological processes secondary to epilepsy.

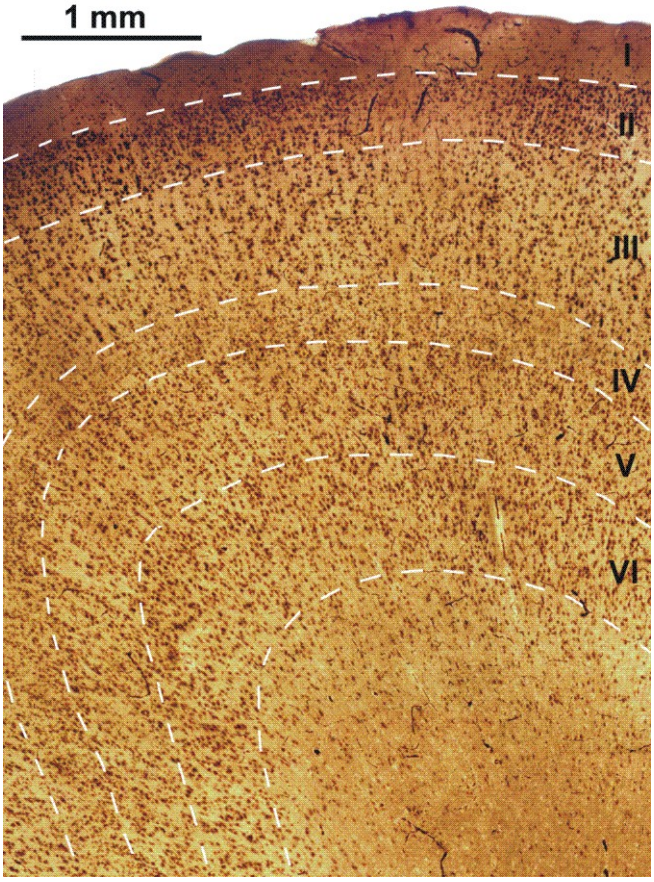

Fig. S1. Example histological exam of tissue immediately adjacent to the electrode tract in Patient G. Microphysiological recordings from this patient are shown in Fig. 3. The neuronal elements and laminar structure are grossly intact. 60-μm-thick section stained with NeuN.

Table S1: Patient characteristics.

Patient	**Gender**	**Age**	**Focus**	**Etiology**
A	M	15	Frontal	Dysplasia
B	F	27	Frontal	Unknown
C	M	39	Temporal	Dysplasia
D	M	16	Frontal	Dysplasia
E	F	18	Temporal	Dysplasia
F	F	48	Parietal	Dysplasia
G	M	35	Frontal	Dysplasia
H	F	34	Frontal	Dysplasia

References

S1. I. Ulbert, E. Halgren, G. Heit, G. Karmos, *Journal of Neuroscience Methods* **106**, 69 (2001).
S2. C. Nicholson, J. A. Freeman, *Journal of Neurophysiology* **38**, 356 (1975).
S3. K. H. Pettersen, A. Devor, I. Ulbert, A. M. Dale, G. T. Einevoll, *J Neurosci Methods* **154**, 116 (2006).
S4. S. Murakami, T. Zhang, A. Hirose, Y. C. Okada, *J Physiol* **544**, 237 (2002).
S5. U. Mitzdorf, *Physiol Rev* **65**, 37 (1985).
S6. J. Holsheimer, *Exp Brain Res* **67**, 402 (1987).
S7. C. Schroeder, A. Mehta, S. Givre, *Cereb Cortex* **8**, 575 (1998).
S8. C. E. Tenke, C. E. Schroeder, J. C. Arezzo, H. G. Vaughan, Jr., *Exp Brain Res* **94**, 183 (1993).
S9. A. Delorme, S. Makeig, *Journal of Neuroscience Methods* **134**, 9 (2004).
S10. E. Halgren, C. Boujon, J. Clarke, C. Wang, P. Chauvel, *Cerebral Cortex* **12**, 710 (2002).
S11. C. Wang, I. Ulbert, D. L. Schomer, K. Marinkovic, E. Halgren, *J Neurosci* **25**, 604 (2005).
S12. A. Rechtschaffen, A. Kales, *A manual of standardized terminology, techniques and scoring system for sleep stages of human subjects*. (US Government Printing Office, Washington,DC, 1968).